Dalton Transactions

Cluster Self-Assembly and Anion Binding by Metal Complexes of Non-Innocent Thiazolidinyl-Thiolate Ligands

Journal:	*Dalton Transactions*
Manuscript ID	DT-COM-04-2022-001339.R2
Article Type:	Communication
Date Submitted by the Author:	07-Jun-2022
Complete List of Authors:	Riffel, Madeline; University of Notre Dame, Siegel, Lukas; University of Notre Dame; Heidelberg University, Chemistry Oliver, Allen; University of Notre Dame, Department of Chemistry and Biochemistry Tsui, Emily; University of Notre Dame,

COMMUNICATION

Cluster Self-Assembly and Anion Binding by Metal Complexes of Non-Innocent Thiazolidinyl-Thiolate Ligands

Madeline N. Riffel,[a] Lukas Siegel,[ab] Allen G. Oliver,[a] and Emily Y. Tsui [a]*

Received 00th January 20xx,
Accepted 00th January 20xx

DOI: 10.1039/x0xx00000x

Zn^{II} and Fe^{II} chloride complexes of a di(methylthiazolidinyl)pyridine ligand were deprotonated to form the corresponding thiolate complexes supported by redox-active iminopyridine moieties. The thiolate donor groups are nucleophilic and reactive toward oxidants, electrophiles, and protons, while the pendant thiazolidine rings are available for hydrogen bonding. Anion exchange with weakly-coordinating triflate anion resulted in self-assembly of the iminopyridine complexes to form a trimeric [M_3S_3] cluster. Hydrogen bonding closely associates anions with this trimetallic core.

Multiple synthetic strategies have been employed for challenging multi-electron and multi-proton transformations. For example, non-innocent ligands facilitate redox and proton-transfer steps for reactions like CO_2 reduction and H_2 evolution.[1-6] Alternatively, multimetallic clusters have been used to accomplish multi-electron processes through cooperative metal-metal interactions or redox processes.[7-8] Combining ligand-non-innocence or other functionality like hydrogen-bonding[9-10] with multimetallic structures is therefore an ongoing effort for more tunable redox behavior and cooperative reactivity.[11-12]

The condensation of aldehydes with 1,2-aminothiol compounds like 2-aminobenzenethiol or cysteamine is known to form thiazolidines rather than imines,[13-15] but in situ deprotonation and metalation yields the corresponding imine-bound metal thiolate complexes.[16-20] While the redox activity of some examples of these complexes has been measured electrochemically,[16] proton-induced transformations of these complexes have not been studied. Here, we report the synthesis of redox-non-innocent and proton-switchable di(2-methylthiazolidinyl)pyridine-supported metal dichloride complexes (M = Zn, Fe). This system shows reversible ring-opening of a methylthiazolidinyl arm into an iminoethanethiolate moiety. Upon counter-ion exchange with triflate, the thiolate complex self-assembles into a trimetallic cluster that can associate anions through hydrogen-bonding interactions.

Di(2-methylthiazolidinyl)pyridine zinc dichloride (**1**, Scheme 1) was prepared in a one-pot reaction by refluxing 2,6-diacetylpyridine, cysteamine hydrochloride (2 equiv), and $Zn(OAc)_2 \bullet 2H_2O$ (1 equiv) in ethanol. Figure 1 shows the solid-state structure obtained by single crystal X-ray diffraction (XRD) of a sample grown by vapor diffusion of hexanes into a THF solution of **1**. The structure shows a C_2-symmetric, 5-coordinate Zn center (τ_5 = 0.47).[21] In solution, however, the ^{1}H NMR spectrum of **1** in d_6-DMSO shows two species in a 1:0.6 ratio (see ESI, Fig. S1); these compounds are assigned as the two diastereomers of **1** caused by the two chiral 2-methylthiazolidinyl substituents. These two sets of ^{1}H NMR signals coalesce at 110 °C in d_6-DMSO (Fig. S4). In $CDCl_3$, the ^{1}H NMR spectrum shows only one set of ligand-centered peaks for one diastereomer (Fig. S2). This solvent dependence is likely due to the different solvent dielectric constants (4.81 for chloroform, 47 for DMSO at 20 °C);[22] as DMSO is more polar, it can stabilize the C_s-symmetric isomer that is expected to exhibit a larger dipole moment.

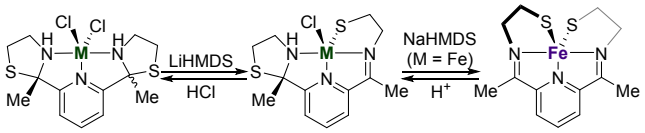

1 (M = Zn) **3** (M = Fe) **2-Cl** (M = Zn) **4-Cl** (M = Fe) **5** (proposed)

Scheme 1 Deprotonation-induced ligand interconversion in Zn and Fe complexes.

Treatment of a DMF solution of **1** with lithium bis(trimethylsilyl)amide (LiHMDS, 1 equiv) deprotonates and ring-opens one 2-methylthiazolidinyl group to form the iminopyridine-supported zinc thiolate monochloride complex **2-Cl** as shown in Scheme 1. Figure 1 shows the XRD structure of

[a] Department of Chemistry and Biochemistry, University of Notre Dame, Notre Dame, IN, USA. E-mail: etsui@nd.edu
[b] Department of Chemistry, Heidelberg University, Heidelberg, Germany
Electronic Supplementary Information (ESI) available: Synthetic procedures and characterization data including NMR spectra, crystallographic details, and electrochemistry data. CCDC 2167681-2167688. See DOI: 10.1039/x0xx00000x

crystals grown by vapor diffusion of diethyl ether into a saturated DMF solution of **2-Cl**. Ring-opening of the thiazolidine group permits relaxation of the Zn geometry to square pyramidal (τ_5 = 0.13). The thiolate moiety of **2-Cl** undergoes reactions typical to other metal thiolate complexes. Addition of methyl iodide to **2-Cl** results in thiolate methylation, as identified by ^{1}H NMR spectroscopy (Fig. S7) and ESI-MS, showing that the thiolate is nucleophilic. Thiolate oxidation by addition of I_2 (0.5 equiv) results in the formation of a mixture of products, presumably due to loss of ZnI_2 upon disulfide formation. Lastly, protonation of **2-Cl** with acids (e.g. HCl) results in ring-closure to regenerate the 2-methylthiazolidinyl group and form **1** (pK_a ~ 10.8) (Fig. S24). This result shows that this ligand can reversibly store protons while remaining coordinated to the metal center.

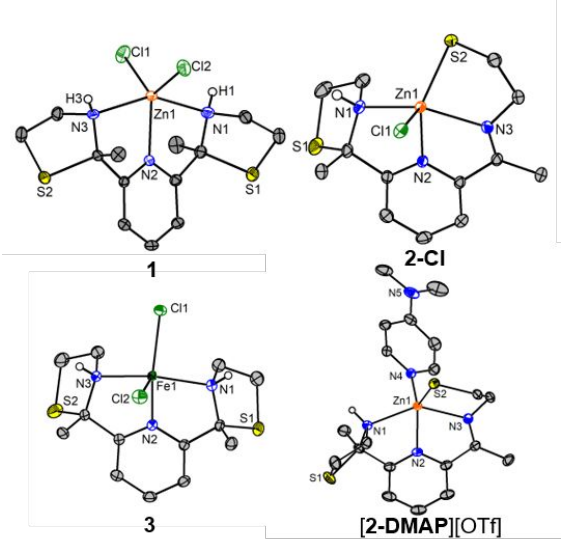

Figure 1 Solid-state structure of monometallic 2-methylthiazolidinylpyridine complexes as 50% thermal ellipsoids. Hydrogen atoms omitted for clarity.

The same synthetic procedures can be extended to other transition metals. The Fe^{II} analog of **1** can be prepared by a similar one-pot condensation of 2,6-diacetylpyridine, cysteamine hydrochloride, and $Fe(OAc)_2$ to yield a pale green solid (**3**, Scheme 1). Deprotonation of **3** forms the putative Fe congener of **2-Cl**, a dark blue compound (**4-Cl**). Compounds **3** and **4-Cl** are paramagnetic, with broadened and shifted ^{1}H NMR resonances. Figure 1 shows the XRD structure of **3**; in contrast to **1**, **3** crystallizes as the C_s-symmetric diastereomer in the solid state, although both diastereomers are observed in the ^{1}H NMR spectrum of a d_6-DMSO solution of **3** (Fig. S16). We have not yet been able to grow X-ray quality single crystals of **4-Cl**, but the ^{1}H NMR spectrum of a d_6-DMSO solution of **4-Cl** is consistent with this assignment (Fig. S17). A solution magnetic susceptibility measurement finds μ_{eff} ~ 3.1 BM, close to the expected spin-only magnetic moment for a S = 1 complex (Evans method).[23]

Attempted deprotonation of **2-Cl** to form a diiminopyridine-supported zinc complex with two thiolate donors formed only an insoluble brown solid, likely a polymeric product in which thiolates bridge between multiple zinc centers. In contrast, treatment of **3** or **4-Cl** with sodium bis(trimethylsilylamide) (NaHMDS, 2 or 1 equiv, respectively) yielded a deep purple product (**5**) that was soluble in benzene and THF (Scheme 1). Although we have been unable to grow X-ray quality single crystals of **5**, the number of ^{1}H NMR signals in the spectrum of a C_6D_6 solution of **5** are consistent with a symmetric product (5 signls, Fig. S18), supporting the proposed deprotonation of the thiazolidinyl ring to form two symmetric iminoethanethiolate arms. Additionally, a comproportionation reaction by mixing equimolar amounts of **5** and **3** in d_6-DMSO formed **4-Cl** (Figs. S31 and S32, Table S1).

Cyclic voltammetry (CV) of the Zn and Fe congeners of these complexes permits distinction between ligand-centered and metal-centered redox processes and therefore analysis of the "redox-non-innocence" of the thiazolidine/iminopyridine ligand frameworks. As expected, the CV of a DMF solution of **1** shows no redox events within the potential range permitted by the solvent, while the CV of **3** shows a Fe^{II}/Fe^{III} oxidation event at $E_{1/2}$ = −0.29 V vs. the ferrocenium/ferrocene redox couple (Fc^+/Fc, Fig. S23). For the iminopyridine-supported complexes, two reductions are observed with $E_{1/2}$ = −1.80 and −1.99 V vs. Fc^+/Fc for **2-Cl** (Fig. S22). These reduction processes are assigned to one- and two-electron reductions of the iminopyridine moiety.[24-25] As such, this ligand framework may provide opportunity for cooperative metal-ligand reactivity in multielectron transformations at potentials accessible by chemical reductants such as Na(Hg) ($E^{o\prime}$ = −2.36 V vs. Fc^+/Fc).[26] The CV of **4-Cl** displays reduction waves around –2 V that are less well-resolved, along with additional metal-centered redox processes that have not yet been completely assigned (Fig. S22). Both **2-Cl** and **4-Cl** also display sulfur-centered thiolate oxidation at positive applied potentials (> 0.6 V vs. Fc^+/Fc).

Anion exchange by treatment of **2-Cl** with Me_3SiOTf (1 equiv) in CH_3CN formed the triflate complex **2-OTf** (Scheme 2). Figure 2 shows the XRD structure of crystals grown by layering diethyl ether on a saturated CH_3CN solution of **2-OTf** at room temperature, showing that the complex crystallizes as a C_3-symmetric trimer ([**6-OTf**]$^{2+}$) where each thiolate S atom bridges two Zn atoms to form a planar six-membered $[Zn_3S_3]$ ring. In this structure, the three 2-methylthiazolidine groups are oriented above the plane of the $[Zn_3S_3]$ ring, and a triflate anion is hydrogen-bonded to the three thiazolidinyl N-H protons, with O(triflate)--N(thiazolidinyl) distances ranging between 2.963(2)–3.048(2) Å. The other two triflate anions remain outer sphere. Similarly, treatment of **4-Cl** with Me_3SiOTf (1 equiv) formed the triiron analog [**7-OTf**]$^{2+}$ (Scheme 2), which was crystallized from THF/hexanes and also shows a hydrogen-bonded triflate anion (Fig. 2).

Thiolate-bridged metal complexes are well-established and have been previously reported as models of bioinorganic metalloenzyme active sites.[27-28] Additionally, similar self-assembly of metal thiolate complexes to form planar trimeric $[M_3S_3]$ species has been previously observed by Holm and co-workers in the study of $[Fe_3S_3]$ clusters supported by simple benzenethiolate ligands.[29] These compounds displayed dynamic behavior in solution to form clusters of other nuclearity via scrambling of thiolate and chloride ligands. This ligand rearrangement is not possible for [**6-OTf**]$^{2+}$ and [**7-OTf**]$^{2+}$, but we considered the possibility that the trimeric structures

dissociate to monomers upon dissolution. To study whether the trimer remains intact in solution, ^{1}H NMR DOSY spectroscopy was used to find the diffusion coefficient of [**6-OTf**]$^{2+}$ in CD_3CN (8.41×10^{-10} m^2/s) (Fig. S28). Using the Stokes-Einstein-Gierer-Wirtz estimation,[30-31] this diffusion constant corresponds to an estimated formula weight (FW) of 1180 g/mol, which is consistent with a trimeric tricationic structure in solution (calcd. 1186.42 g/mol for [**6-OTf**]$^{2+}$). We note that this estimate does not account for the solvent shell associated with the tricationic structure. Although the trimeric structure is stable to the addition of Lewis bases like MeOH and PMe_3, it dissociates upon addition of DMSO or more nucleophilic bases such as pyridine (py), butylamine, or 4-dimethylaminopyridine (DMAP) (Figs. S26, S27). ^{1}H NMR DOSY spectroscopy of the DMAP complex [**2-DMAP**][OTf] in CD_3CN measured a higher diffusion coefficient of 1.3×10^{-9} m^2/s (Fig. S30), consistent with a monomeric structure with estimated FW 590 g/mol (calcd. 467.98 g/mol for [**2-DMAP**]$^+$). Figure 1 shows the XRD structure of crystals grown by vapor diffusion of diethyl ether into a saturated CH_3CN solution of [**2-DMAP**][OTf] at 0°C.

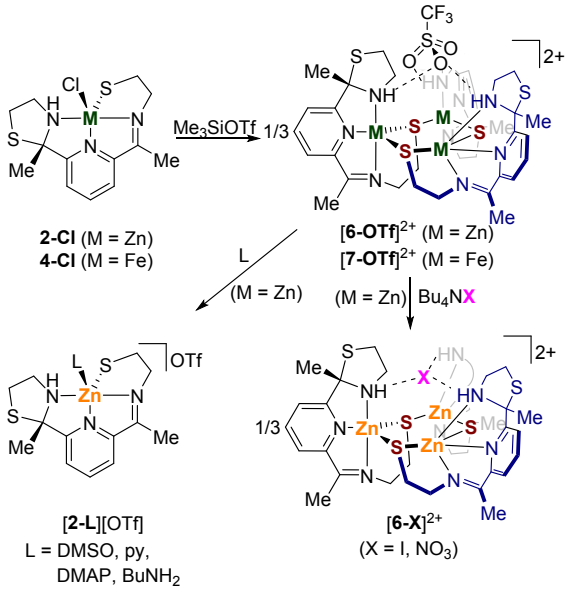

Scheme 2 Self-assembly of trimeric structures upon chloride abstraction with trimethylsilyl triflate. Strong Lewis bases result in cluster dissociation, while weaker Lewis bases and anions can coordinate to the trimer via hydrogen bonding.

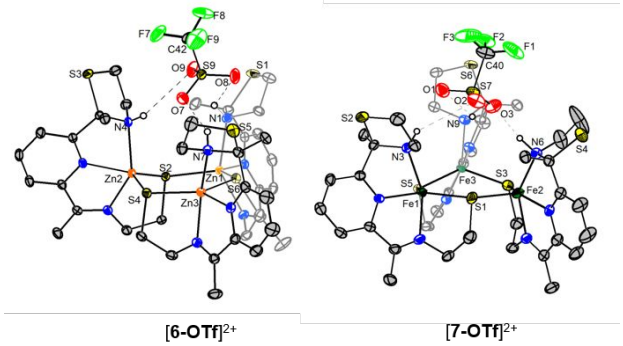

Figure 2 Solid-state structures of trimeric [M_3S_3] complexes as 50% thermal ellipsoids. Hydrogen atoms and outer-sphere triflate anions omitted for clarity.

Spectroscopy of [**7-OTf**]$^{2+}$ provides additional support for the assignment that these complexes retain their trimeric structure in acetonitrile. In CD_3CN, the magnetic susceptibility of [**7-OTf**]$^{2+}$ per Fe center shows a μ_{eff} ~ 2.2 BM, lower than the expected spin-only magnetic moment of an Fe^{II}, d^6, S = 2 complex. This value may suggest antiferromagnetic coupling between Fe centers via the bridging thiolate atoms, as observed with other Fe^{II}–(μ_2-S)–Fe^{II} bridged species.[29, 32] Additionally, the electronic absorption spectrum of [**7-OTf**]$^{2+}$ in CH_3CN shows shifted bands from those of **4-Cl** (Fig. S21). Addition of DMAP to this acetonitrile solution results in DMAP coordination and trimer dissociation, and a shift in the absorption spectrum to more closely match that of **4-Cl**. Taken together, these data are consistent with strong M–(μ_2-S)–M interactions in solutions of [**6-OTf**]$^{2+}$ and [**7-OTf**]$^{2+}$.

We next investigated the solution behavior of the hydrogen-bonded anion observed in the solid-state structure of [**6-OTf**]$^{2+}$. A CD_3CN solution of [**6-OTf**]$^{2+}$ was treated with increasing amounts of Bu_4NI (0.17–3 equiv/trimer). The ^{1}H NMR signal corresponding to the 2-methylthiazolidine N-H proton (δ_{NH}) shifts with increasing [I^-], demonstrating displacement of a coordinated triflate anion and binding of iodide to form [**6-I**]$^{2+}$ (Scheme 2 and Fig. 3). ^{1}H NMR DOSY of [**6-I**]$^{2+}$ (Fig. S29) showed a diffusion coefficient of 8.1×10^{-10} m^2/s, consistent with a trimeric structure with an estimated FW 1280 g/mol (calcd. 1164.33 g/ mol for [**6-I**]$^{2+}$). Further addition of iodide (> 1 equiv/trimer) does not continue to shift the NMR signal, as the hydrogen-bonding "pocket" can only accommodate one anion. Instead, at these high iodide concentrations, a yellow precipitate formed that is assigned as the monomeric complex **2-I** with zinc-bound iodide, as confirmed by XRD (Fig. 4). Although layering ether over an acetonitrile solution of [**6-I**]$^{2+}$ formed colorless needles proposed to be the anion-exchanged trimer, they have been unfortunately too fine for single crystal X-ray diffraction.

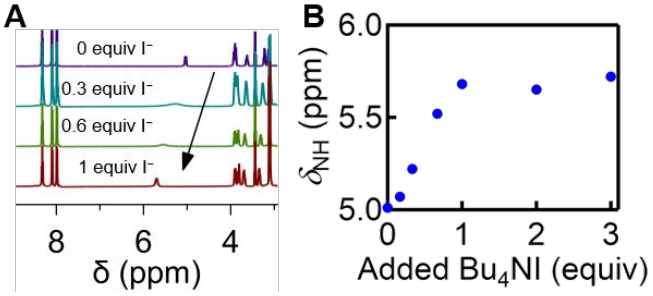

Figure 3 (A) ^{1}H NMR spectra of a CD_3CN solution of [**6-OTf**]$^{2+}$ treated with increasing concentrations of Bu_4NI (0–1 equiv), showing a downfield shift in the thiazolidine NH ^{1}H NMR signal (δ_{NH}) . (B) δ_{NH} (ppm) vs. added equivalents of Bu_4NI.

Other polyatomic anions can also exchange with triflate and hydrogen bond to the thiazolidine ligand moieties. Treatment of acetonitrile solutions of [**6-OTf**]$^{2+}$ with [Bu_4N][NO_3] followed by removal of [Bu_4N][OTf] by THF extraction forms the corresponding [**6-NO$_3$**]$^{2+}$ complex in which a nitrate anion is hydrogen-bonded to the complex rather than triflate. The ^{1}H NMR spectrum of [**6-NO$_3$**]$^{2+}$ shows a similar downfield shift of the thiazolidine proton from [**6-OTf**]$^{2+}$ (Fig. S33). However, addition of excess [Bu_4N][NO_3] does not result in trimer

dissociation, likely due to the weaker coordination of nitrate to Zn^{2+}. XRD of crystals grown by vapor diffusion of diethyl ether into an acetonitrile solution of $[\mathbf{6\text{-}NO_3}]^{2+}$ confirms this assignment (Fig. 4). In this structure, the nitrate is hydrogen-bonded to the thiazolidine rings, as expected, with O(nitrate)--N(thiazolidinyl) distances of 2.899(3)–2.996(4) Å. This complex is of particular interest because hydrogen-bonding to nitrate has been studied in the design of molecular receptors[33] as well as in the context of electrocatalytic nitrate reduction for environmental remediation.[34-35]

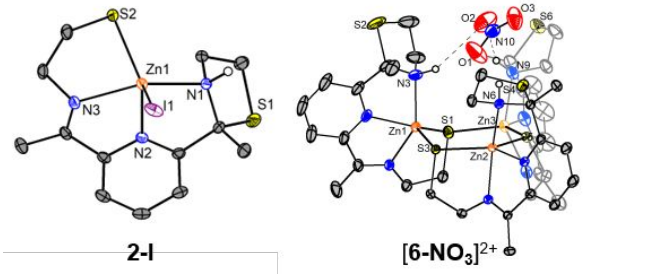

Figure 4 Solid-state structures of **2-I** and $[\mathbf{6\text{-}NO_3}]^{2+}$ as 50% thermal ellipsoids. Hydrogen atoms and outer-sphere anions omitted for clarity.

In conclusion, we have shown that the di(2-methylthiazolidinyl)pyridine ligand framework can support first-row transition metals and can also accommodate one or two deprotonation events to form the resulting thiolate-bound iminopyridine- and diiminopyridine-supported complexes. As such, this framework can be both proton-active and, in its iminopyridine and diiminopyridine forms, redox-active. Further, the (2-methylthiazolidinyl)iminopyridine structure can self-assemble in solution to form trimeric structures that show strong bridging sulfur interactions. These structures loosely associate anions near the trimeric core via hydrogen-bonding interactions. Studies are underway to target these structures as platforms for multi-electron multi-proton transformations.

This work was funded by NSF CHE-2047045. Financial support from the German Academic Exchange Service (Fellowship for L.S. through the ISAP program) is gratefully acknowledged. We thank Dr. Evgenii Kovrigin for assistance with NMR experiments and Dr. Mijoon Lee for assistance with mass spectrometry.

Conflicts of interest

There are no conflicts to declare.

Notes and references

1 A. Chapovetsky, T. H. Do, R. Haiges, M. K. Takase, S. C. Marinescu, *J. Am. Chem. Soc.*, 2016, **138**, 5765-5768.
2 M. L. Helm, M. P. Stewart, R. M. Bullock, M. R. DuBois, D. L. DuBois, *Science*, 2011, **333**, 863-866.
3 J. F. Hull, Y. Himeda, W.-H. Wang, B. Hashiguchi, R. Periana, D. J. Szalda, J. T. Muckerman, E. Fujita, *Nat. Chem.*, 2012, **4**, 383-388.
4 G. W. Margulieux, M. J. Bezdek, Z. R. Turner, P. J. Chirik, *J. Am. Chem. Soc.*, 2017, **139**, 6110-6113.
5 C. A. Lippert, S. A. Arnstein, C. D. Sherrill, J. D. Soper, *J. Am. Chem. Soc.*, 2010, **132**, 3879-3892.
6 V. Lyaskovskyy, B. de Bruin, *ACS Catal.*, 2012, **2**, 270-279.
7 T. M. Powers, T. A. Betley, *J. Am. Chem. Soc.*, 2013, **135**, 12289-12296.
8 G. L. Guillet, F. T. Sloane, D. M. Ermert, M. W. Calkins, M. K. Peprah, E. S. Knowles, E. Čižmár, K. A. Abboud, M. W. Meisel, L. J. Murray, *Chem. Commun.*, 2013, **49**, 6635-6637.
9 E. W. Dahl, J. J. Kiernicki, M. Zeller, N. K. Szymczak, *J. Am. Chem. Soc.*, 2018, **140**, 10075-10079.
10 J. P. Shanahan, N. K. Szymczak, *J. Am. Chem. Soc.*, 2019, **141**, 8550-8556.
11 D. Wang, S. V. Lindeman, A. T. Fiedler, *Inorg. Chem.*, 2015, **54**, 8744-8754.
12 S. Zhang, P. Cui, T. Liu, Q. Wang, T. J. Longo, L. M. Thierer, B. C. Manor, M. R. Gau, P. J. Carroll, G. C. Papaefthymiou, N. C. Tomson, *Angew. Chem. Int. Ed.*, 2020, **59**, 15215-15219.
13 A. W. Hofmann, *Ber.*, 1880, **13**, 1223-1238.
14 M. T. Bogert, A. Stull, *J. Am. Chem. Soc.*, 1925, **47**, 3078-3083.
15 M. T. Bogert, B. Naiman, *J. Am. Chem. Soc.*, 1935, **57**, 1529-1533.
16 P. Ghosh, E. Bill, T. Weyhermüller, F. Neese, K. Wieghardt, *J. Am. Chem. Soc.*, 2003, **125**, 1293-1308.
17 K. Henrick, R. W. Matthews, P. A. Tasker, *Inorg. Chim. Acta*, 1977, **25**, L31-L32.
18 L. F. Lindoy, D. H. Busch, *Inorg. Chem.*, 1974, **13**, 2494-2498.
19 L. F. Lindoy, D. H. Busch, V. Goedken, *J. Chem Soc., Chem. Commun.*, 1972, 683-684.
20 S. Y. Shaban, R. Puchta, R. v. Eldik, *Z. Naturforsch B*, 2010, **65**, 251-257.
21 A. W. Addison, T. N. Rao, J. Reedijk, J. van Rijn, G. C. Verschoor, *J. Chem. Soc., Dalton Trans.*, 1984, 1349-1356.
22 C. Wohlfahrt *2 Pure Liquids: Data: Datasheet from Landolt-Börnstein - Group Iv Physical Chemistry · Volume 6: "Static Dielectric Constants of Pure Liquids and Binary Liquid Mixtures" in Springermaterials (Https://Doi.Org/10.1007/10047452_2)*, Springer-Verlag Berlin Heidelberg.
23 D. F. Evans, *J. Chem. Soc.*, 1959, 2003-2005.
24 G. M. Duarte, J. D. Braun, P. K. Giesbrecht, D. E. Herbert, *Dalton Trans.*, 2017, **46**, 16439-16445.
25 S. Sharma, G. A. Andrade, S. Maurya, I. A. Popov, E. R. Batista, B. L. Davis, R. Mukundan, N. C. Smythe, A. M. Tondreau, P. Yang, J. C. Gordon, *Energy Storage Mater.*, 2021, **37**, 576-586.
26 N. G. Connelly, W. E. Geiger, *Chem. Rev.*, 1996, **96**, 877-910.
27 D. Sellmann, W. Prechtel, F. Knoch, M. Moll, *Inorg. Chem.*, 1993, **32**, 538-546.
28 E. Almaraz, Q. A. de Paula, Q. Liu, J. H. Reibenspies, M. Y. Darensbourg, N. P. Farrell, *J. Am. Chem. Soc.*, 2008, **130**, 6272-6280.
29 M. A. Whitener, J. K. Bashkin, K. S. Hagen, J. J. Girerd, E. Gamp, N. Edelstein, R. H. Holm, *J. Am. Chem. Soc.*, 1986, **108**, 5607-5620.
30 R. Evans, G. Dal Poggetto, M. Nilsson, G. A. Morris, *Anal. Chem.*, 2018, **90**, 3987-3994.
31 R. Evans, Z. Deng, A. K. Rogerson, A. S. McLachlan, J. J. Richards, M. Nilsson, G. A. Morris, *Angew. Chem. Int. Ed.*, 2013, **52**, 3199-3202.
32 A. P. Ginsberg, M. E. Lines, K. D. Karlin, S. J. Lippard, F. J. DiSalvo, *J. Am. Chem. Soc.*, 1976, **98**, 6958-6966.
33 B. P. Hay, M. Gutowski, D. A. Dixon, J. Garza, R. Vargas, B. A. Moyer, *J. Am. Chem. Soc.*, 2004, **126**, 7925-7934.
34 C. L. Ford, Y. J. Park, E. M. Matson, Z. Gordon, A. R. Fout, *Science*, 2016, **354**, 741-743.

35 H.-Y. Kwon, S. E. Braley, J. P. Madriaga, J. M. Smith, E. Jakubikova, *Dalton Trans.*, 2021, **50**, 12324-12331.